Polarization angle dependence of the breathing mode in confined one-dimensional dipolar bosons

S. De Palo [1,2] E. Orignac [3] M. L. Chiofalo [4,5] and R. Citro [6,7,*]

[1]*CNR-IOM-Democritos National Simulation Centre, UDS, Via Bonomea 265, I-34136, Trieste, Italy*
[2]*Dipartimento di Fisica Teorica, Università Trieste, Strada Costiera 11, I-34014 Trieste, Italy*
[3]*Université de Lyon, Ens de Lyon, Université Claude Bernard, CNRS, Laboratoire de Physique, F-69342 Lyon, France*
[4]*Dipartimento di Fisica, Università di Pisa, I-56126 Pisa, Italy*
[5]*INFN sezione di Pisa, Largo Bruno Pontecorvo 3, I-56126 Pisa (Italy)*
[6]*Dipartimento di Fisica "E. R. Caianiello," Università degli Studi di Salerno and CNR-Spin, Via Giovanni Paolo II, I-84084 Fisciano (Sa), Italy*
[7]*Gruppo Collegato di Salerno, INFN-Sezione di Napoli, I-84084 Fisciano, Salerno, Italy*

(Received 13 December 2020; revised 14 February 2021; accepted 16 February 2021; published 4 March 2021)

Probing the radial collective oscillation of a trapped quantum system is an accurate experimental tool to investigate interactions and dimensionality effects. We consider a fully polarized quasi-one-dimensional dipolar quantum gas of bosonic dysprosium atoms in a parabolic trap at zero temperature. We model the dipolar gas with an effective quasi-one-dimensional Hamiltonian in the single-mode approximation and derive the equation of state using a variational approximation based on the Lieb-Liniger gas Bethe ansatz wave function or perturbation theory. We calculate the breathing mode frequencies while varying polarization angles by a sum-rule approach and find they are in good agreement with recent experimental findings.

DOI: 10.1103/PhysRevB.103.115109

I. INTRODUCTION

Systems with long-range interactions present a host of exotic quantum states of matter, including Wigner crystals [1,2], Haldane insulators [3], and Fulde-Ferrell-Larkin-Ovchinnikov phases [4], thanks to the interplay between quantum fluctuations and the frustrating effects of interactions. In particular, the advent of degenerate quantum gases consisting of atoms in which strong dipolar forces provide the interactions has even revealed the coexistence of both crystalline order and superfluidity, the so-called supersolidity [5–7].

Recently, the possibility of forming one-dimensional tubes of bosonic Dy atoms with tunable strength of the contact and dipolar interactions [8] opened the fascinating perspective of investigating the interplay between quantum fluctuations, enhanced in reduced dimensionality, and interaction-driven fluctuations, leading to unconventional relaxation mechanisms and the so-called scar states [9]. In fact, although in one dimension repulsive dipolar interaction decaying as $1/r^3$ at long distance is classified as finite-range interaction, it is expected to push bosonic systems to a regime of stronger interactions [10–12].

Since the majority of existing ultracold-gas experiments are carried out with spatially inhomogeneous systems, due to the presence of an external confining potential, exciting oscillations of the gas density distribution in such a confined geometry have been demonstrated to be a reliable, basic tool for investigating the spectrum of collective excitations and the phase diagram [13–15].

From this perspective, one-dimensional (1D) gases show their own peculiarities [16,17]. A paradigmatic example is the exactly solvable Lieb-Liniger gas [18], in which at infinite contact interaction strength $g_{1D} \to \infty$ the many-body excitation spectrum becomes identical to that of a free Fermi gas, known as the Tonks-Girardeau gas [19]. The presence of an external parabolic potential renders the low-lying part of the excitation spectrum discrete, where the simplest mode to be excited among the low-lying ones after small instantaneous changes in the trapping frequency ω_z is the so-called breathing (or compressional) mode, i.e., the uniform radial expansion and contraction of the system. The breathing mode frequency ω_b depends on the interaction strength g_{1D}, the number of particles N in the trap, and the gas temperature T. It was previously shown that the frequency ratio ω_b/ω_z presents two crossovers as a function of increasing interaction: from a value of 2 down to $\sqrt{3}$ while going from the noninteracting to weakly interacting regime and then back to 2 after crossing towards the strongly interacting limit [20]. Theoretical descriptions based on the local density approximation [16], time-dependent Hartree method [21], and diffusion Quantum Monte Carlo simulations [22] have been produced following the system across the different regimes.

Here, we focus on the breathing mode of a one-dimensional dipolar quantum gas and investigate the influence of both the dipole orientation and the interplay between zero (contact) and finite-range (dipolar) interaction allowing for independent tuning of these two interactions. Our analysis is based on a sum-rule approach [16] that allows us to extract the breathing mode frequency from ground-state density profiles obtained after solving the stationary generalized Gross-Pitaevskii equation. The latter is generalized by replacing the Hartree term with the energy per unit length of the bulk quasi-one-

*Corresponding author: rocitro@unisa.it

dimensional dipolar system, obtained using either a Bethe ansatz wave function in a variational calculation [23] or a perturbative approach.

The results show that when dipolar interactions are attractive, the system manifests an incipient instability at low density, and a sharp minimum is found in the breathing mode which is very peculiar of that finite-range interaction. In the repulsive regime an extension of the stability regime is instead observed. Good agreement with the experimental results reported in Refs. [9,24] is also found.

This paper is organized as follows. We introduce the model Hamiltonian and the generalized Gross-Pitaevskii equation in Sec. II. Then in Sec. III we discuss the equation of state by separating the short-range terms from the soft dipolar long-range interaction in the single-mode approximation. In Sec. IV we present the results for the breathing mode by discussing the case of the repulsive and attractive interactions, following the evolution of this quantity after varying the dipole orientation θ in the whole range from 0 to $\pi/2$. Finally, in Sec. V we give conclusions and discuss perspectives.

II. THE MODEL AND THE GENERALIZED GROSS-PITAEVSKII EQUATION

In highly elongated traps the atomic motion in the plane transverse to the longitudinal direction is described by the Hamiltonian

$$H_\perp = \frac{p_x^2 + p_y^2}{2m} + \frac{m\omega_\perp^2}{2}(x^2 + y^2), \tag{1}$$

where m is the mass particle and $\omega_\perp$ is the confining harmonic oscillator frequency. When the frequency $\omega_\perp \gg \omega_{ho}$ is sufficiently larger than the longitudinal trapping frequency ω_{ho}, the many-body wave function of the atoms can be projected on the ground-state manifold of the Hamiltonian (1) [25]. This is the so-called single-mode approximation.

The effective Hamiltonian in the projected subspace depends only on the coordinates along the z axis. Its expression is [26,27]

$$H_{1D} = -\frac{\hbar^2}{2m}\sum_i \frac{\partial^2}{\partial z_j^2} + g_{1D}\sum_{i<j}\delta(z_i - z_j) + \sum_i V_{ext}(z_i) + \sum_{i<j} V_{Q1D}(z_i - z_j), \tag{2}$$

where $V_{ext}(z) = \frac{1}{2}m\omega_{ho}^2 z^2$ is the potential energy of the parabolic trap along the longitudinal z direction, g_{1D} is the contact interaction coming from van der Waals or other short-range interactions, and the effective one-dimensional (1D) dipole-dipole interaction $V_{Q1D}(z)$ in the single-mode approximation reads [26]

$$V_{Q1D}(z/l_\perp) = V(\theta)\left[V_{DDI}^{1D}\left(\frac{z}{l_\perp}\right) - \frac{8}{3}\delta\left(\frac{z}{l_\perp}\right)\right], \tag{3}$$

where

$$V(\theta) = \frac{\mu_0\mu_D^2}{4\pi}\frac{1 - 3\cos^2\theta}{4l_\perp^3} \tag{4}$$

encodes the sign and the effective strength of the interaction driven by the vacuum magnetic permeability μ_0, the magnetic dipolar moment μ_D of the given atomic species, the angle θ between the dipole orientation and the longitudinal z axis, and the transverse oscillator length $l_\perp = \sqrt{\hbar/(m\omega_\perp)}$. The adimensional form of the effective 1D dipolar potential V_{DDI}^{1D} is

$$V_{DDI}^{1D}\left(\frac{z}{l_\perp}\right) = -2\left|\frac{z}{l_\perp}\right| + \sqrt{2\pi}\left[1 + \left(\frac{z}{l_\perp}\right)^2\right] \times e^{\left(\frac{z}{l_\perp}\right)^2/2}\mathrm{erfc}\left[\left|\frac{z}{\sqrt{2}l_\perp}\right|\right]. \tag{5}$$

In the ^{162}Dy case relevant to current experiments [9], $\mu_D = 9.93\ \mu_B$ [8].

At zero temperature, the Gross-Pitaevskii theory [28–30] provides a good description of weakly interacting three-dimensional atomic Bose-Einstein condensates, yet it requires modifications either with strong interactions or reduced dimensionality. In the original form, without dipolar interaction, the energy functional in the Gross-Pitaevskii approximation is [28,29]

$$F_{GP} = \int dz\left[\frac{\hbar^2}{2m}\nabla\phi\nabla\phi^* + [V_{ext}(z) - \mu]|\phi|^2 + \frac{g_{1D}}{2}|\phi|^4\right] \tag{6}$$

where $\phi(z,t)$ is the Bose-Einstein condensate order parameter, $n(z,t) = |\phi(z,t)|^2$ is the boson density, and μ is the chemical potential. In one dimension and in the case of hard-core bosons [19], Kolomeisky *et al.* proposed a modification of the Gross-Pitaevskii equation to describe the Tonks-Girardeau regime [31], where the Hartree term $g_{1D}|\phi|^4/2$ is replaced by the energy density of the hard-core boson (or free spinless fermion [19,32]) gas, i.e., $\hbar^2\pi^2|\phi|^6/(6m)$. Such an approach can be viewed as taking the classical limit in the bosonized Hamiltonian of spinless fermions with quadratic dispersion [33]. Afterwards, different proposals [25,34,35] were offered to cover both the weakly and strongly interacting regimes; one of them amounts to replacing the Hartree term with an energy-density functional [25,34] for the Lieb-Liniger gas that interpolates between the Hartree and Tonks-Girardeau limits (see Appendix A). Indeed, in one dimension, the Lieb-Liniger gas is integrable by the Bethe ansatz technique [18,36], and an exact expression of the ground-state energy as a function of the boson density is available.

The ground-state energy density of the Lieb-Liniger gas reads

$$e_{LL}(n) = \frac{\hbar^2}{2m}n^3\epsilon_{LL}(n), \tag{7}$$

where $\epsilon_{LL}(n)$ is an adimensional function that can be obtained from the Bethe ansatz solution [37–39]. Using the ground-state energy (7) in the generalized Gross-Pitaevskii equation (GPE) has been shown to reproduce [34] the results of the hydrodynamic approach [16,17] for the lowest breathing mode (see Appendix A for details).

Along these lines, in this work we replace the Hartree term in the Gross-Pitaevskii equation (6) with the energy per unit length of the bulk quasi-one-dimensional dipolar system

$$e(n) = \frac{\hbar^2}{2m}n^3\epsilon(n), \tag{8}$$

where $\epsilon(n)$ is obtained using either a Bethe Ansatz wave function in a variational calculation [23] or a perturbative approach that we detail in the next section.

The approximation to the energy functional now reads

$$F_{GP}=\int dz\left[\frac{\hbar^2}{2m}\nabla\phi\nabla\phi^*+[V_{\rm ext}(z)-\mu]|\phi|^2+e(|\phi|^2)\right] \quad (9)$$

yielding the equation of motion [34,35] for $\phi(z,\tau)$, $i\hbar\partial_\tau\phi=\delta F_{GP}/\delta\phi^*$, i.e.,

$$i\hbar\partial_\tau\phi=\left[-\frac{\hbar^2\nabla^2}{2m}+[V_{\rm ext}(z)-\mu]+\frac{1}{\phi}\frac{\delta e(|\phi|^2)}{\delta\phi^*}\right]\phi, \quad (10)$$

with the wave function normalized to the number N of atoms in the trap, $N=\int dz|\phi(z)|^2$.

III. EQUATION OF STATE

We start our analysis by recalling the method used in Ref. [8] to reduce the system with dipolar interaction (3) to an integrable Lieb-Liniger model. First, in the Hamiltonian (2) all the short-range contact interactions are isolated. Then, besides the van der Waals $g_{\rm 1D}$ and the contact interaction in Eq. (2), a contact term $AV(\theta)$ that effectively accounts for the short-range part of the interaction $V^{\rm 1D}_{DDI}(r)$ is added. The effective Lieb-Liniger Hamiltonian reads

$$H^{LL}_{Q1D}=-\frac{\hbar^2}{2m}\sum_i\frac{\partial^2}{\partial x_i^2}+\left[g_{\rm 1D}+V(\theta)(A-\frac{8}{3})l_\perp\right]\sum_{i<j}\delta(x_i-x_j), \quad (11)$$

where the normalized strength of the short-range part of the interaction can be approximately taken as $A=\int_{-\sqrt{2\pi}}^{+\sqrt{2\pi}}duV^{\rm 1D}_{DDI}(u)\simeq 3.6$ in the single-mode approximation and independently of the density of atoms [8]. The nonzero A takes care of the shortest-range part ($|z|<\sqrt{2\pi}l_\perp$) of the dipolar potential (5), leaving the longer-range $\sim 1/z^3$ integrability-breaking tail as a possible perturbation.

Taking $A=0$ would amount to neglecting the short-range part of the dipolar interaction (5) and thus approximate repulsive or attractive dipolar interactions with an attractive or repulsive contact interaction, respectively [26]. Obviously, such an approximation is unphysical. The effect of making $A>0$ is to counterbalance the attractive contact term coming from the single-mode approximation. When $A>8/3$, stability is enlarged in the repulsive case, while in the attractive case instability can be obtained for $g_{\rm 1D}$ not sufficiently repulsive.

A reliable estimate of A can be determined via a variational Bethe ansatz (VBA) wave function approach [23], in which, for each density, this effective contact interaction is determined by the minimization of the energy per particle using the Bethe ansatz wave function of the Lieb-Liniger model as a trial wave function.

The dimensionless coupling γ for the Lieb-Liniger Hamiltonian defined in (11) is

$$\gamma=\frac{1}{n}\frac{m}{\hbar^2}g_{Q1D}(\theta)=\frac{2}{na_{Q1D}}$$

$$=\frac{2}{n}\left[-\frac{1}{a_{\rm 1D}}+\frac{a_d}{l_\perp^2}\frac{1-3\cos\theta^2}{4}\left(A-\frac{8}{3}\right)\right], \quad (12)$$

where $g_{\rm 1D}=-2\hbar^2/(ma_{\rm 1D})$ and $a_d=\mu_0\mu_D^2m/(8\pi\hbar^2)$ is the dipolar length. In this work we will focus on the region where $a_{\rm 1D}<0$, so that the contact interaction strength $g_{\rm 1D}$ is positive.

In previous modelizations [8], the basic assumptions were that (i) A was independent of the density and the scattering length $a_{\rm 1D}$ and (ii) the tail of the dipolar interaction was negligible. To start with, let us include the tail of $V^{\rm 1D}_{DDI}(z/l_\perp)$ by means of a perturbative approach.

We write the original Hamiltonian (2) as the sum of the integrable Lieb-Liniger Hamiltonian (11) and a correction term δV,

$$H=H^{LL}_{Q1D}(\gamma)+\sum_{i<j}\delta V(z_i-z_j), \quad (13)$$

$$\delta V(z)=V(\theta)\left[V^{\rm 1D}_{DDI}(z/l_\perp)-Al_\perp\delta(z)\right]. \quad (14)$$

In order to estimate the effect of the interaction $\delta V(z)$, we resort to perturbation theory (PT). In particular, we will consider two benchmark values for A, $A=3.6$ as in Ref. [8] and $A=0$, which amounts to treating the whole $V(\theta)[V^{\rm 1D}_{DDI}(z/l_\perp)]$ at the perturbative level. At first order, the energy per N particles is

$$\frac{E_{pt}}{N}=\epsilon_{pt}(n)\simeq\frac{E_{LL}(\gamma)}{N}+\frac{n}{2}\int dz\delta V(z)g_{LL}(z), \quad (15)$$

with E_{LL} being the Lieb-Liniger ground-state energy for the Hamiltonian (11) evaluated at γ, while $g_{LL}(z)$ is the pair correlation function [40,41] of the Lieb-Liniger gas. Using (15), we obtain an equation of state $e_{\rm PT}(n)$ that depends on the chosen A, in addition to $a_d/l_\perp$, $|a_{\rm 1D}|/l_\perp$, and θ. We remark that in our perturbation theory, the perturbative term in (15) is chosen so that its weight is only 10% of the total weight of the dipolar interaction [8]. This ensures the validity of the approximation.

In the rest of the paper, we compare the results obtained with the following three approximations for the equation of state: $\varepsilon_{LL}(n)$, perturbation theory based on (15) with $A=3.6$, and the variational Bethe ansatz as in Ref. [23], which gives a variational estimate of the ground-state energy independent of the approximation [8] chosen for A. For comparison, we will also show the results for the most unfavorable case obtained when the whole dipolar part is treated in perturbation theory, that is, $A=0$.

In Fig. 1 we show the energies $\epsilon(n)$ within three different approximations: $\epsilon_{LL}(n)$ using Eq. (11) and $A=3.6$, $\epsilon_{\rm PT}(n)$ with $A=3.6$, and, finally, the variational Bethe ansatz. Results are shown for three selected scattering lengths, $a_{\rm 1D}=-100a_0$, $-1000a_0$, and $-5000a_0$, and for $\theta=\pi/2$, i.e., for repulsive interaction. We choose $a_d=195a_0$, $l_\perp=57.3$ nm, and $a_{ho}=24\,000a_0$ to make contact with recent experimental works [8,9]. For small scattering lengths, the equations of state from the perturbative approach using $A=3.6$ and from the variational Bethe ansatz are in good agreement with each other. Equations of state within these two approximations visibly depart from ϵ_{LL} based on Eq. (11) at small and intermediate densities and on increasing the scattering length,

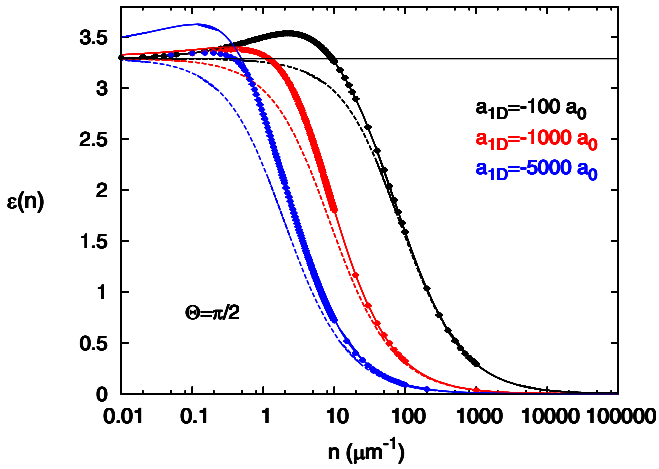

FIG. 1. Energy per unit length $\epsilon(n)$ in units of $\hbar^2 n^3/(2m)$ within three different approximations: $\epsilon_{LL}(n)$ with $A = 3.6$ (dashed lines), perturbation theory using $A = 3.6$ (solid lines), and the variational Bethe ansatz (solid dots). The results are shown for three selected scattering lengths, $a_{1D} = -100a_0, -1000a_0$, and $-5000a_0$, the black, red, and blue data, respectively, and for $\theta = \pi/2$.

as expected since the dipolar interactions become more dominant.

The typical situation for the attractive interaction, i.e., for $\theta = 0$, is displayed in Fig. 2, where we show the data for $a_{1D} = -1000a_0$ and $-5000a_0$ and compare the energy results coming from variational Bethe ansatz and perturbation theory using $A = 3.6$ for all densities and $A = 0.0$, that is, treating the whole dipolar interaction as a perturbation. At low and intermediate densities, energies obtained within PT with $A = 0$ largely deviate from VBA results and within themselves. Only at very large densities do these differences decrease, and results from PT with $A = 0$ are closer to the variational

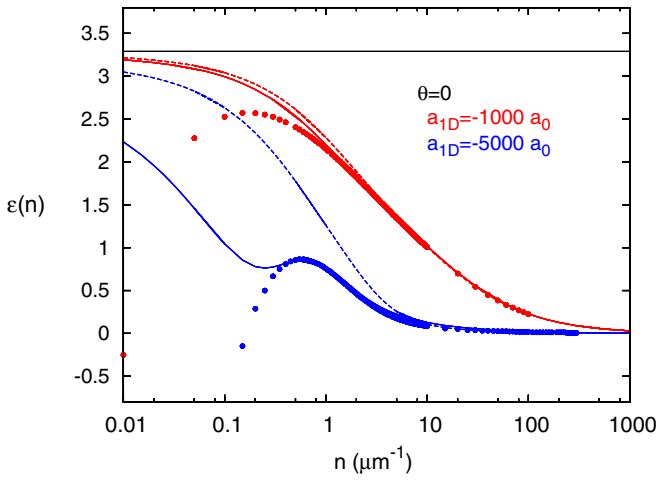

FIG. 2. Energy per unit length $\epsilon(n)$ in units of $\hbar^2 n^3/(2m)$ within three different approximations: using perturbation theory with $A = 3.6$ (solid lines) and using $A = 0.0$ (dashed lines) compared with those within the variational Bethe ansatz (solid dots). Data are shown for two selected scattering lengths, $a_{1D} = -1000a_0$ and $-5000a_0$, represented by the red and blue data points, respectively. Results are for $\theta = 0$.

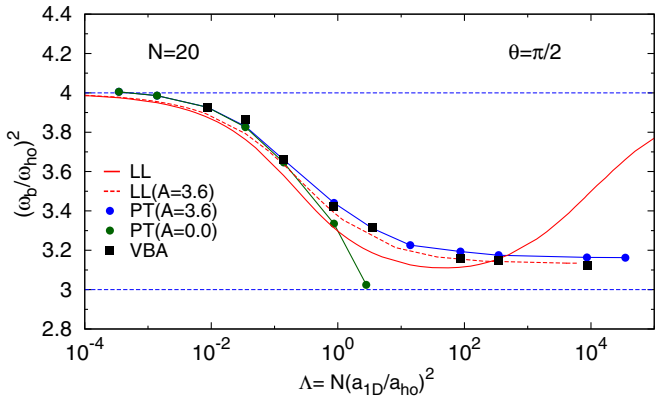

FIG. 3. Squared breathing mode frequency over trapping frequency squared ω_b^2/ω_{ho}^2 as a function of $\Lambda = N(a_{1D}/a_{ho})^2$, using different approximations. All results are for $N = 20$, and lines are only a guide to the eyes. Red, dark-green, and blue solid curves are estimates using the Lieb-Liniger model and the perturbation theory with $A = 0$ and with $A = 3.6$, respectively. The dashed red curve represents ω_b^2/ω_{ho}^2 calculated using Eq. (11) with $A = 3.6$. the black solid squares are estimates based on the variational Bethe ansatz equation of state.

results. It should be kept in mind that those differences are strongly reduced by the n^3 factor in the energy per volume $E/V = n^3\epsilon(n)$.

These results emphasize that using a single effective contact interaction A, independent of both density and scattering length, can yield an inaccurate equation of state, especially with attractive dipolar interactions. The VBA approach, by optimizing the parameter A to minimize the ground-state energy, takes care of these uncertainties. The relevance of such differences for the calculation of the breathing mode frequency in a trapped system will be considered in the next section.

IV. THE BREATHING MODE

We evaluate the frequency of the lowest radial compressional oscillation by a sum-rule approach [16] that allows us to compute the breathing mode frequency from ground-state density profiles obtained by solving the stationary generalized Gross-Pitaevskii equation using standard imaginary-time evolution algorithms [42]. The breathing mode ω_b is obtained as the response of the gas to a change in the trap frequency ω_{ho}:

$$\omega_b^2 = -2\left\langle \sum_{i=1}^{N} z_i^2 \right\rangle \left[\frac{\partial \left\langle \sum_{i=1}^{N} z_i^2 \right\rangle}{\partial \omega_{ho}^2} \right]^{-1}. \tag{16}$$

It is convenient (see Appendix B) to study the evolution of the breathing mode as a function of $\Lambda = Na_{1D}^2/a_{ho}^2$, with N being the number of particles in the trap. By solving the time-dependent generalized Gross-Pitaevskii equation, we have verified that, after initially exciting the mode by external radial compression of the trap, in the limit $|a_{1D}| \to 0$, $(\omega_b/\omega_{ho})^2 = 4$.

We estimate the breathing mode using the different approximations described above, starting from the case $\theta = \pi/2$ (see Fig. 3).

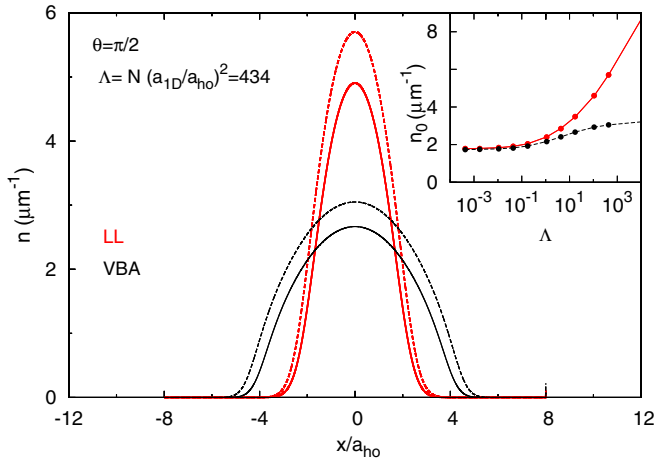

FIG. 4. Density profile for a system of N dipoles in a trap using two different equations of states at $\Lambda = 434$, namely, the Lieb-Liniger (LL) (red lines) and VBA (black lines). Dashed and solid lines refer to the cases with $N = 25$ and $N = 20$ particles in the trap, respectively. Results are for $\theta = \pi/2$. In the inset, we show the density at the center of the trap as a function of Λ for $N = 25$; the red and black solid dots represent estimates using the LL and VBA equations of state, respectively. Lines joining dots are only a guide to the eye.

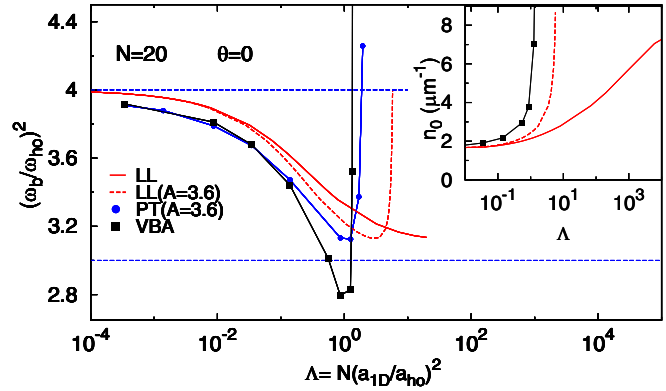

FIG. 5. Squared breathing mode frequency over trapping frequency squared ω_b^2/ω_{ho}^2 as a function of $\Lambda = N(a_{1D}/a_{ho})^2$, using different approximations. The red solid and dashed lines represent the breathing mode estimates after using the Lieb-Liniger (LL) model without dipolar interaction and using $A = 3.6$ in Eq. (11), respectively. Blue solid curves refer to estimates based on the perturbation theory with $A = 3.6$, while black solid squares are based on the variational Bethe ansatz (VBA). All results are for $N = 20$, and lines are only guides to the eye. In the inset, the density at the center of the trap is shown as a function of Λ, with the same legend as in the main panel.

In the region of small scattering lengths $|a_{1D}|$, the breathing modes are dominated by the van der Waals repulsive contact interaction, and dipolar interactions are marginally relevant: all the approximations, even completely neglecting the dipolar interaction, predict similar results. On increasing $|a_{1D}|$, apart from using PT with $A = 0$ that fails when $g_{Q1D}(\pi/2)$ becomes negative, all the other approximations shown in Fig. 3 are very close to each other. The important effect of dipolar interaction becomes visible for very large $|a_{1D}|$ values, where it enlarges the region of stability, and for $|a_{1D}| \to \infty$, the breathing mode frequency reaches a plateau. This behavior can already be obtained within the approximation of [8] since with $A = 3.6$, according to Eq. (11), $g_{Q1D}(\pi/2)$ saturates in that limit.

We note that when $\Lambda < 10^3$, the estimates of the breathing mode frequency from both the PT using $A = 3.6$ and the VBA are compatible with the one obtained by dropping the dipolar interaction entirely. This last modelization, however, would predict that the breathing mode reaches the noninteracting limit at large $\Lambda > 10^4$, i.e., $(\omega_b/\omega_{ho})^2 \to 4$, at variance with the other two approximations that predict a plateau at a lower $(\omega_b/\omega_{ho})^2 \simeq 3.2$, hinting at the persistence of interactions.

At large $|a_{1D}|$, even when the predictions for the breathing mode are all compatible, we can trace a difference in the density profile, as illustrated in Fig. 4 at $\Lambda = 434$, where we show it using the VBA and Lieb-Liniger (LL) model.

Using either $\epsilon_{\rm VBA}(n)$ or $\epsilon_{\rm PT}(A = 3.6, n)$ yields a density at the center of the trap that ranges from $\simeq$2.6 to 3.1 μm^{-1} (see the black curves in the main panel of Fig. 4), while the density value at the center of the trap is almost doubled for the Lieb-Liniger gas without dipolar interaction described by $\epsilon_{LL}(n)$. The first estimates are in agreement with the averaged density at the center of trap as measured in Ref. [8]. In the inset we show the variation of the density at the center of the trap as a function of Λ for the Lieb-Liniger equation of state and the VBA. The values become notably different for $\Lambda \gtrsim 10$, whereas (see Fig. 3) the behavior of the breathing mode becomes qualitatively different for the two approximations only for $\Lambda \gtrsim 500$. The behavior of the density profiles shows that the physics of the system at large scattering lengths is different in the presence of repulsive dipolar interactions and could be used as a sensitive indicator together with the frequency of the breathing mode.

Turning to the attractive case, i.e., $\theta = 0$, on increasing $|a_{1D}|$ the $g_{Q1D}(\theta)$ in Eq. (12) rapidly becomes small and negative, and the key issue is to what extent the system of the dipolar gas is still stable against possible collapse [43], the formation of a solitonic/droplet phase [35], or a gas/droplet coexistence [44]. The predictions for the breathing modes are qualitatively different from the repulsive case since both the VBA and the estimates with $A = 3.6$, with or without correction to first order, predict that for $\Lambda > 2$ the breathing mode rapidly decreases to reach a minimum with $\omega_b^2/\omega_0^2 < 3$, after which it rapidly increases until the overall effective interaction becomes negative. Due to negative g_{Q1D}, the LL model using $A = 3.6$ [Eq. (11)] also predicts an instability but at a higher value of Λ than the two other approximations with $3 < \omega_b^2/\omega_{ho}^2 < 4$.

The important discrepancy for $\Lambda > 1$ between the $A = 3.6$ approximation and its first-order correction suggests a breakdown of this approximation. If we contrast the latter with the VBA, we observe that VBA predicts a deeper minimum of the breathing mode frequency than the $A = 3.6$ approximation, even with first-order corrections. Comparing the densities at the center of the trap (see the inset of Fig. 5), we note that differences in density are becoming noticeable already for $\Lambda \sim 0.1$, suggesting again that the density profile is more sensitive to the presence of dipolar interaction than the breathing

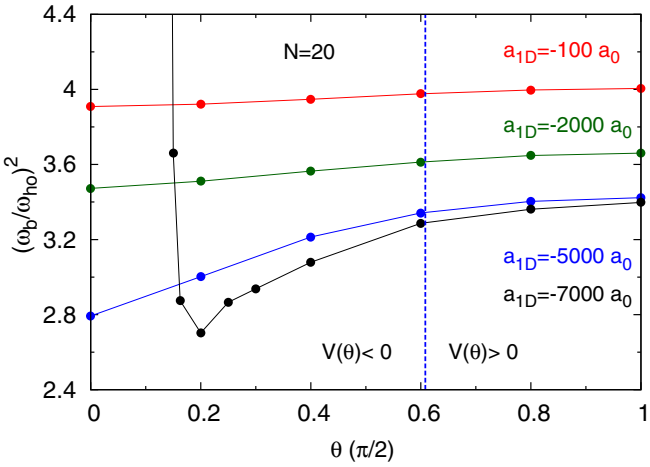

FIG. 6. Squared breathing mode frequency over trapping frequency squared ω_b^2/ω_{ho}^2 as a function of the polarization angle θ for selected values of the scattering length, $a_{1D}/a_0 = -100, -2000, -5000, -7000$, represented by red, dark-green, blue, and black solid dots, respectively. The solid lines joining the data are only guides to the eye. The vertical blue dashed line splits the regions with negative $V(\theta) < 0$ (left) and positive $V(\theta) > 0$ (right). Data refer to estimates based on the variational Bethe ansatz equation of state.

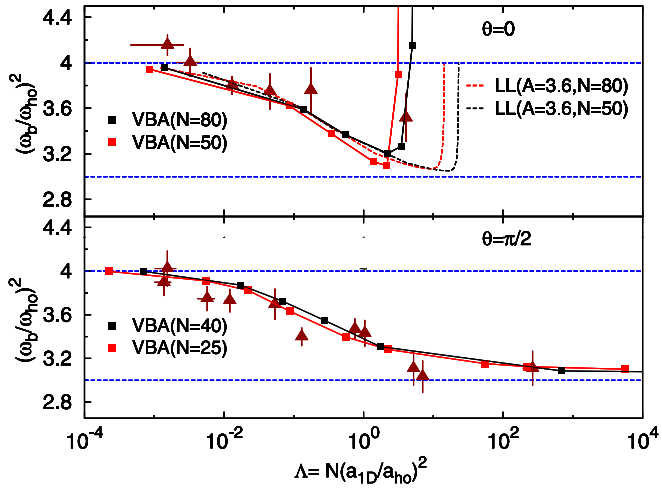

FIG. 7. Squared breathing mode frequency over trapping frequency squared ω_b^2/ω_{ho}^2 as a function of $\Lambda = N(a_{1D}/a_{ho})^2$, using different approximations, for the attractive case (top panel) and the repulsive one (bottom panel). Dark-red triangles represent the experimental data taken from Refs. [9,24]. All results are shown for two values of N, $N = 50, 80$ (top panel) and $N = 25, 40$ (bottom panel), and lines are only a guide to the eyes. The dashed black and red lines represent estimates using the Lieb-Liniger model. Black and red solid squares are estimates based on the variational Bethe ansatz (VBA) equation of state.

mode. In any case, all the approximations confirm that we are approaching an instability at intermediate values of $\Lambda \sim 1$. Of course, only a direct comparison with experimental data could permit us to identify which approximation is the most suitable for other predictions, as we will see later on.

Comparing the repulsive and attractive cases, we see that attractive dipolar interactions produce stronger qualitative effects on the behavior of the breathing mode or on the density profile at a given a_{1D}. In addition, differences between the VBA and the perturbation theory with $A = 3.6$ are also more significant in the presence of repulsive interactions. Such an observation is in agreement with the behavior of the energy density represented in Figs. 1 and 2, where the differences between the approximations manifest themselves for lower $|a_{1D}|$ in the attractive case.

Having analyzed the physics of the breathing mode in the two extreme cases of maximally repulsive and attractive dipolar interactions, we are now in a position to discuss the dependence on the polarization angle. We show in Fig. 6 the effect of changing the polarization angle θ while keeping the scattering length $|a_{1D}|$ fixed. For a large range of scattering lengths the effect of varying the angle is very small and visible only just before the system becomes unstable. For the largest scattering length and attractive interaction, the breathing mode rapidly grows, signaling the instability, as previously found.

We conclude our discussion by contrasting the proposed approximation with the experimental data from Ref. [9,24], as shown in Fig. 7. We note that for the repulsive case ($\theta = \pi/2$) all the experimental points are in very good agreement with the VBA prediction with both $N = 25$ and $N = 40$, which are the minimum and maximum numbers of particles in the trap characterizing the experiment. Our findings suggest that for $\Lambda \geqslant 1$ the dipolar interaction is efficient in enhancing the region of stability of the interacting regime and in inhibiting the increase of the breathing mode frequency towards the noninteracting limit. The agreement with the VBA predictions is also confirmed for the attractive case ($\theta = 0$) where the curve with $N = 80$ and $N = 50$ agrees well with the experimental points. The comparison with the LL theory, using $A = 3.6$ and neglecting the tail interaction [Eq. (11)], clearly shows that despite its correct qualitative behavior the VBA description is needed to make contact with experimental findings. The comparison with the experiments clearly indicates that the system crosses over an instability point for Λ of the order 1. Whether this instability is due to the formation of simple bound states [43] or droplet formation [35] needs further investigations, in particular from the experimental point of view. Here, additional data in the interval Λ between 10^{-1} and 1 for $\theta = 0$ would, indeed, help to provide a quantitative test for the existence of the predicted minimum and to assess its nature. For $\Lambda > 10$, experiments did not succeed at evidencing a stable condensate [24].

V. CONCLUSIONS

In conclusion, we have considered the energy density of a gas of dipolar bosons in a tight transverse trapping using either the approximation of Ref. [8], supplemented by first-order perturbation theory, or a variational approximation [23]. We have found that in the case of repulsive dipolar interactions, the three approaches are in good agreement with each other. We have used energy densities under different approximations to predict the breathing mode frequencies of the trapped dipolar gas. When dipolar interactions become attractive, the results of the two approximations become quite

different, especially at low density. This gives rise to notable differences in the frequency of the breathing mode, with the variational method giving a stronger dip before the instability. In all cases, observing the effect of the dipolar interaction requires us to weaken the contact interaction that is competing with it enough. In comparison to experimental results, we have shown that the variational predictions are especially compatible with the present measurements [9,24]. However, except in the attractive case, the experimental results are also compatible with a pure contact interaction.

As already noticed in our previous work [10], this can be considered further proof that, for all relevant purposes, the nature of $1/r^3$ power-law interactions in one dimension, in the ground-state repulsive branch, can be viewed as short-range interactions [45]. It would be worthwhile for future experiments to attempt to explore the region with $\Lambda > 400$ in the repulsive regime, where deviations for the pure contact interaction are expected, and the range $0.1 < \Lambda < 1$ in the attractive case, where deviations from the pure contact interaction are maximal, and the difference between the two approximations considered here is the most visible.

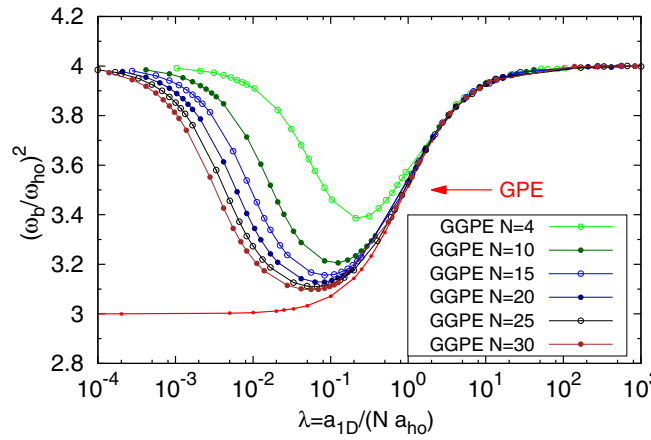

FIG. 8. Ratio of breathing mode frequency to trap frequency squared ω_B^2/ω_{ho}^2 as a function of the Hartree parameter λ for different numbers of particles in the trap, namely, $N = 4$, 10, 15, 20, 25, and 30, using the generalized Gross-Pitaevskii equation (A2). The red solid line represents the Hartree approximation, independent of the number of particles.

ACKNOWLEDGMENTS

We thank B. Lev and his group for enlightening discussions and for private communication of data and C. Menotti for useful discussions.

APPENDIX A: GENERALIZED GROSS-PITAEVSKII EQUATION FOR THE LIEB-LINIGER TRAPPED SYSTEM

We replace the Hartree term in Eq. (6) with the ground-state density energy of the Lieb-Liniger gas equation (7), so that the energy functional and the equation of motion read

$$F_{GP} = \int dz \left[\frac{\hbar^2}{2m} |\nabla\phi|^2 + V_{\rm ext}(z)|\phi|^2 + e(|\phi|^2) \right], \tag{A1}$$

$$i\hbar\partial_\tau \phi = \left[-\frac{\hbar^2\nabla^2}{2m} + V_{\rm ext}(z) + \frac{1}{\phi}\frac{\delta e(|\phi|^2)}{\delta\phi^*} \right]\phi, \tag{A2}$$

where

$$\frac{1}{\phi}\frac{\delta e(n)}{\delta\phi^*} = \frac{\hbar^2}{2m}\left[3n^2\epsilon_{LL}(\gamma[n]) - \frac{2n}{a_{\rm 1D}}\frac{d\epsilon_{LL}(\gamma[n])}{d\gamma} \right], \tag{A3}$$

with $\epsilon_{LL}(\gamma[n])$ being the adimensional ground-state density energy functional for the Lieb-Liniger gas, for example, from Refs. [37–39]. We use a normalized wave function as well as harmonic-oscillator units, which means that lengths and energies are, respectively, expressed in units of a_{ho} and $\hbar\omega_{ho}$, so that

$$n = \frac{N}{a_{ho}}|\psi|^2, \tag{A4}$$

$$\gamma = \frac{2a_{ho}}{N|\phi|^2 a_{\rm 1D}} = \frac{2}{N^2\lambda|\psi|^2}, \tag{A5}$$

$$\lambda = \frac{a_{\rm 1D}}{Na_{ho}}, \tag{A6}$$

where λ is the Hartree parameter. In these units, Eq. (A3) becomes

$$\frac{1}{\phi}\frac{\delta e(n)}{\delta\phi^*} = \frac{3}{2}N^2|\psi|^4\epsilon(\gamma[n]) - \frac{1}{\lambda}|\psi|^2\epsilon'(\gamma[n]), \tag{A7}$$

and it covers the strong- and weak-interaction cases. Indeed, in the weak-interaction limit

$$\lim_{\gamma\to 0}\frac{1}{\phi}\frac{\delta e(n)}{\delta\phi^*} \to \frac{3}{\lambda}|\psi|^2 - \frac{1}{\lambda}|\psi|^2 = \frac{2}{\lambda}|\psi|^2,$$

we recover the usual Gross-Pitaevskii equation

$$i\hbar\partial_t\psi = \left[\frac{1}{2}(-\nabla^2 + x^2) + \frac{2}{\lambda}|\psi|^2 \right]\psi, \tag{A8}$$

while in the strong-interaction limit

$$\lim_{\gamma\to\infty}\frac{1}{\phi}\frac{\delta e(n)}{\delta\phi^*} \to \frac{3}{2}N^2|\psi|^4\epsilon(\gamma[n]) = \frac{\pi^2}{2}N^2|\psi|^4,$$

we get back to the proposal from Kolomeisky *et al.* [31] to describe the Tonks-Girardeau gas,

$$i\hbar\partial_t\psi = \left[\frac{1}{2}(-\nabla^2 + x^2) + \frac{\pi^2}{2}N^2|\psi|^2|\psi|^2 \right]\psi. \tag{A9}$$

Results for the breathing modes using this approach for different numbers of particles in the trap are shown in Fig. 8 and compared with the usual Gross-Pitaevskii equation.

APPENDIX B: BREATHING MODE OF AN INHOMOGENEOUS TOMONAGA-LUTTINGER LIQUID

Here, we briefly recall the relevant parameters to study the evolution of the breathing mode in a trapped Tomonaga-Luttinger liquid [11,16,17]. The Hamiltonian of the inhomogeneous Tomonaga-Luttinger liquid reads

$$H = \int_{-R}^{R}\frac{dx}{2\pi}\hbar\left[u(x)K(x)(\pi\Pi)^2 + \frac{u(x)}{K(x)}(\partial_x\phi)^2 \right], \tag{B1}$$

where [11]

$$u(x)K(x) = \frac{\hbar\pi\rho(x)}{m}, \tag{B2}$$

$$\frac{u(x)}{K(x)} = \frac{1}{\pi\hbar}\left(\frac{\partial\mu}{\partial\rho}\right)_{\rho=\rho(x)}, \tag{B3}$$

with $\rho(x)$ being the density of atoms at position x, μ being the chemical potential, m being the mass of a single atom, and $2R$ being the dimension of the trapped atomic cloud. Using the equations of motion method, one obtains [11,16,17]

$$\partial_t^2\phi = u(x)K(x)\partial_x\left(\frac{u(x)}{K(x)}\partial_x\phi\right) \tag{B4}$$

$$= \frac{\rho(x)}{m}\partial_x\left(\frac{\partial\mu}{\partial\rho}\partial_x\phi\right). \tag{B5}$$

The breathing modes are obtained by looking for solutions of (B4) of the form $\phi(x,t) = \phi_n(x)e^{i\omega_n t}$ subject to the boundary conditions $\phi_n(\pm R) = 0$. The local chemical potential in a harmonic trap is fixed by the equation

$$\mu(\rho(x)) = \tfrac{1}{2}m\omega_0^2(R^2 - x^2). \tag{B6}$$

In the case of the Lieb-Liniger gas, the energy per unit length is given by (8),

$$e(\rho) = \frac{\hbar^2\rho^3}{m}\bar{\epsilon}(\rho a_{1D}); \tag{B7}$$

therefore, it is convenient to use a reduced density $\nu(x) = a_{1D}\rho(x)$ and write $\mu(\rho) = \partial_\rho e(\rho)$ in the form

$$\mu = \frac{\hbar^2}{ma_{1D}^2}\psi(\nu), \tag{B8}$$

so that after inverting (B6) we find

$$\nu = \psi^{-1}\left(\frac{a_{1D}^2(R^2 - x^2)}{a_{ho}^4}\right), \tag{B9}$$

where we have introduced the trapping length $a_{ho} = \sqrt{\hbar/(m\omega_0)}$. If we consider the total number of particles N, we have

$$N = \int_{-R}^{R}\rho(x)dx, \tag{B10}$$

and injecting (B9), we find that

$$\frac{Na_{1D}}{R} = \int_{-1}^{1}du\psi^{-1}\left(\frac{a_{1D}^2R^2(1-u^2)}{a_{ho}^4}\right). \tag{B11}$$

Solving that equation yields

$$R = \frac{a_{ho}^2}{a_{1D}}G(\Lambda), \tag{B12}$$

with $\Lambda = Na_{1D}^2/a_{ho}^2$. Introducing the dimensionless variable $\xi = a_{1D}x/a_{ho}^2$, we can rewrite the density and the chemical potential in the form

$$\rho(x) = a_{1D}^{-1}F_1[G(\Lambda)^2 - \xi^2], \tag{B13}$$

$$\partial_\rho\mu(\rho(x)) = \frac{\hbar^2}{ma_{1D}}F_2[G(\Lambda)^2 - \xi^2] \tag{B14}$$

and obtain the dimensionless eigenvalue equation

$$F_1[G(\Lambda)^2 - \xi^2]\partial_\xi\{F_2[G(\Lambda)^2 - \xi^2]\partial_\xi\phi_n\} = -(\omega_n/\omega_0)^2\phi_n, \tag{B15}$$

with boundary conditions $\phi_n[\xi = \pi G(\Lambda)] = 0$. So in the case of the Lieb-Liniger gas the eigenvalues $(\omega_n/\omega_0)^2$ depend only on the parameter Λ. Obviously, this is not going to be the case in the dipolar gas where the ground-state energy per unit length also depends on the dimensionless ratios a_{1D}/a_d and $a_{1D}/l_\perp$ and the angle θ. However, in a limit where the dipolar interaction can be replaced by an effective contact interaction, the same kind of scaling will hold.

[1] H. J. Schulz, Phys. Rev. Lett. **71**, 1864 (1993).
[2] S. Capponi, D. Poilblanc, and T. Giamarchi, Phys. Rev. B **61**, 13410 (2000).
[3] E. G. Dalla Torre, E. Berg, and E. Altman, Phys. Rev. Lett. **97**, 260401 (2006).
[4] X. Wei, C. Gao, R. Asgari, P. Wang, and G. Xianlong, Phys. Rev. A **98**, 023631 (2018).
[5] L. Tanzi, E. Lucioni, F. Famà, J. Catani, A. Fioretti, C. Gabbanini, R. N. Bisset, L. Santos, and G. Modugno, Phys. Rev. Lett. **122**, 130405 (2019).
[6] F. Böttcher, J.-N. Schmidt, M. Wenzel, J. Hertkorn, M. Guo, T. Langen, and T. Pfau, Phys. Rev. X **9**, 011051 (2019).
[7] L. Chomaz, D. Petter, P. Ilzhöfer, G. Natale, A. Trautmann, C. Politi, G. Durastante, R. M. W. van Bijnen, A. Patscheider, M. Sohmen, M. J. Mark, and F. Ferlaino, Phys. Rev. X **9**, 021012 (2019).
[8] Y. Tang, W. Kao, K.-Y. Li, S. Seo, K. Mallayya, M. Rigol, S. Gopalakrishnan, and B. L. Lev, Phys. Rev. X **8**, 021030 (2018).
[9] W. Kao, K.-Y. Li, K.-Y. Lin, S. Gopalakrishnan, and B. L. Lev, Science **371**, 296 (2021).
[10] R. Citro, E. Orignac, S. De Palo, and M.-L. Chiofalo, Phys. Rev. A **75**, 051602(R) (2007).
[11] R. Citro, S. De Palo, E. Orignac, P. Pedri, and M. Chiofalo, New J. Phys. **10**, 045011 (2008).
[12] T. Roscilde and M. Boninsegni, New J. Phys. **12**, 033032 (2010).
[13] M.-O. Mewes, M. R. Andrews, N. J. van Druten, D. M. Kurn, D. S. Durfee, C. G. Townsend, and W. Ketterle, Phys. Rev. Lett. **77**, 988 (1996).
[14] D. S. Jin, J. R. Ensher, M. R. Matthews, C. E. Wieman, and E. A. Cornell, Phys. Rev. Lett. **77**, 420 (1996).
[15] A. Altmeyer, S. Riedl, C. Kohstall, M. J. Wright, R. Geursen, M. Bartenstein, C. Chin, J. H. Denschlag, and R. Grimm, Phys. Rev. Lett. **98**, 040401 (2007).
[16] C. Menotti and S. Stringari, Phys. Rev. A **66**, 043610 (2002).
[17] D. Petrov, D. Gangardt, and G. Shlyapnikov, J. Phys. IV **116**, 3 (2004).
[18] E. H. Lieb and W. Liniger, Phys. Rev. **130**, 1605 (1963).
[19] M. Girardeau, J. Math. Phys. **1**, 516 (1960).
[20] E. Haller, M. Gustavsson, M. Mark, J. G. Danzl, R. Hart, H. C. Naegerl, and G. Pupillo, Science **325**, 1224 (2009).

[21] R. Schmitz, S. Krönke, L. Cao, and P. Schmelcher, Phys. Rev. A **88**, 043601 (2013).
[22] A. I. Gudyma, G. E. Astrakharchik, and M. B. Zvonarev, Phys. Rev. A **92**, 021601(R) (2015).
[23] S. De Palo, R. Citro, and E. Orignac, Phys. Rev. B **101**, 045102 (2020).
[24] B. Lev (private communication).
[25] V. Dunjko, V. Lorent, and M. Olshanii, Phys. Rev. Lett. **86**, 5413 (2001).
[26] F. Deuretzbacher, J. C. Cremon, and S. M. Reimann, Phys. Rev. A **81**, 063616 (2010); **87**, 039903(E) (2013).
[27] S. Sinha and L. Santos, Phys. Rev. Lett. **99**, 140406 (2007).
[28] L. P. Pitaevskii, Zh. Eksp. Teor. Fiz. **40**, 646 (1961) [Sov. Phys. JETP **13**, 451 (1961)] .
[29] E. P. Gross, J. Math. Phys. **4**, 195 (1963).
[30] L. Pitaevskii and S. Stringari, *Bose-Einstein Condensation* (Clarendon, Oxford, 2003).
[31] E. B. Kolomeisky, T. J. Newman, J. P. Straley, and X. Qi, Phys. Rev. Lett. **85**, 1146 (2000).
[32] A. Minguzzi, P. Vignolo, M. L. Chiofalo, and M. P. Tosi, Phys. Rev. A **64**, 033605 (2001).
[33] E. Bettelheim, A. G. Abanov, and P. B. Wiegmann, J. Phys. A **41**, 392003 (2008).
[34] P. Öhberg and L. Santos, Phys. Rev. Lett. **89**, 240402 (2002).
[35] R. Ołdziejewski, W. Górecki, K. Pawłowski, and K. Rzaążewski, Phys. Rev. Lett. **124**, 090401 (2020).
[36] E. H. Lieb, Phys. Rev. **130**, 1616 (1963).
[37] G. Lang, F. Hekking, and A. Minguzzi, SciPost Phys. **3**, 003 (2017).
[38] Z. Ristivojevic, Phys. Rev. B **100**, 081110(R) (2019).
[39] M. Marino and T. Reis, J. Stat. Phys. **177**, 1148 (2019).
[40] J.-S. Caux and P. Calabrese, Phys. Rev. A **74**, 031605(R) (2006).
[41] A. Yu. Cherny and J. Brand, Phys. Rev. A **79**, 043607 (2009).
[42] R. K. Kumar, L. E. Young-S., D. Vudragovic, A. Balaz, P. Muruganandamd, and S. Adhikari, Comput. Phys. Commun. **195**, 117128 (2015).
[43] J. B. McGuire, J. Math. Phys. **5**, 622 (1964).
[44] Y. Kora and M. Boninsegni, Phys. Rev. A **101**, 023602 (2020).
[45] M. Dalmonte, G. Pupillo, and P. Zoller, Phys. Rev. Lett. **105**, 140401 (2010).